Research Square

Preprints are preliminary reports that have not undergone peer review.
They should not be considered conclusive, used to inform clinical practice,
or referenced by the media as validated information.

Effect Of Shot Peening On The Microstructural And Mechanical Properties Of As-Built 316l Stainless Steel Printed By WAAM-CMT Additive Manufacturing

Samir Adjel
Moustafa Boukraa
boukraamostafa@yahoo.fr

CRTI: Centre de Recherche en Technologies Industrielles https://orcid.org/0000-0001-6449-8336
Andrian Permana
Syed Haris Iftikhar
Neçar Merah
Fadi Al-Badour2
Tawfiq Chekifi
Atef Chibani

Research Article

Keywords: WAAM-CMT, SS 316L, Shot peening, Residual stress, tensile test, Microstructure, Microhardness, SEM fractography

Posted Date: June 12th, 2026

DOI: https://doi.org/10.21203/rs.3.rs-9932639/v1

License: This work is licensed under a Creative Commons Attribution 4.0 International License.
Read Full License

Effect Of Shot Peening On The Microstructural And Mechanical Properties Of As-Built 316l Stainless Steel Printed By WAAM-CMT Additive Manufacturing

Samir Adjel[1], Moustafa Boukraa[1,*], Andrian Permana[2], Syed Haris Iftikhar[3], Neçar Merah[2, 3], Fadi Al-Badour[2,3], Tawfiq Chekifi [4], Atef Chibani[1].

[1] Research Center in Industrial Technologies CRTI, P.O.Box 64, Cheraga 16014, Algiers, Algeria.
[2] Department of Mechanical Engineering, King Fahd University of Petroleum and Minerals, Dhahran 31261, Saudi Arabia.
[3] Interdisciplinary Research Center for Advanced Materials, King Fahd University of Petroleum & Minerals, Dhahran, 31261, Saudi Arabia.
[4] Unité de Recherche Appliqué en Energies Renouvelables, URAER, Centre de Développement des Energies Renouvelables, CDER, 47133, Ghardaïa, Algeria

Abstract

Wire Arc Additive Manufacturing using the Cold Metal Transfer process (WAAM-CMT) is a promising technique for producing medium- and large-scale stainless-steel components with high deposition efficiency and relatively low heat input. However, WAAM-fabricated 316L materials may still exhibit surface irregularities, thermal-cycle-induced microstructural heterogeneity, and anisotropic mechanical behavior. In this work, flat walls of 316L austenitic stainless steel were fabricated by WAAM-CMT. Tensile, microstructural, microhardness, SEM-based fractography and EDX analyses were conducted on specimens before and after shot peening. In the as-built condition, the bottom region showed the highest ultimate strength (UTS ≈ 480 MPa) but lower ductility (≈ 32 %), while the middle and top exhibited lower strength (UTS ≈ 420 MPa) and higher elongation (≈ 40 %). After shot peening, strength became more uniform across the wall (UTS ≈ 470–490 MPa) with reduced elongation (~25 %). Microstructural observations revealed general grain refinement and surface strengthening, with ferrite and pearlite-like grains significantly refined at most positions. Microhardness increased in all regions due to plastic deformation, grain refinement, and compressive residual stresses introduced by shot peening. SEM fractography revealed ductile fracture behavior dominated by micro-void coalescence in both conditions. EDX analysis confirmed that shot peening did not significantly change the chemical composition of the WAAM-CMT 316L stainless steel. Overall, shot peening effectively enhanced surface hardness and strength uniformity in WAAM-CMT 316L stainless steel.

Keywords: WAAM-CMT, SS 316L, Shot peening, Residual stress, tensile test, Microstructure, Microhardness, SEM fractography.

Corresponding author *: boukraamostafa@yahoo.fr. ORCID: 0000-0001-6449-8336 Research Center in Industrial Technologies CRTI, Cheraga, P.O. Box 64, 16014 Algiers, Algeria

1. Introduction

Wire Arc Additive Manufacturing (WAAM), particularly when combined with Cold Metal Transfer (CMT), has emerged as a cost-effective and versatile technique for producing large-scale metallic components with excellent mechanical performance **[1-4]**. The WAAM uses an electric arc as a heat source to melt the wire feed stock and deposit it layer-by-layer to produce the 3D parts with the precise movement of a welding torch **[5-8]** . Researchers use different types of arc sources such as gas metal arc welding (GMAW), plasma arc welding (PAW), and gas tungsten arc welding (GTAW) to fabricate the components using the WAAM process **[9-11]**. This technology is mostly advantageous in fabricating large, complex stainless steel structures for industries such as aerospace **[5]**, marine engineering **[12]**, and ressure vessel components **[13].** Among the materials suited to this process, austenitic stainless steel 316L is of industrial interest because of its corrosion resistance, high toughness, and weldability **[5, 9, 14-16]**. Recent investigations have demonstrated that WAAM-CMT can reliably fabricate defect-free 316L structures whose microstructure and properties rival or surpass those of conventionally wrought counterparts**[17]** . Typical builds show fine equiaxed grains near the substrate, transitioning to columnar austenite dendrites and skeletal or lathy ferrite toward the top layers. The robust deposition rates and flexibility of this technology have positioned it as a promising alternative to traditional manufacturing methods, particularly for producing medium to large structural components**[18]**. However, the successful application of WAAM depends on the precise control of several parameters that influence the quality of the final product, which makes ongoing research in this area critical **[19, 20]**.

The microstructure and mechanical properties of WAAM-CMT 316L stainless steel are strongly influenced by processing parameters such as welding current, travel speed, gas flow rate, wire feed rate, and contact tip-to-work distance. Kishor et al. **[1]** reported that travel speed, current, and gas flow rate significantly affect the tensile strength and hardness of WAAM-CMT 316L stainless steel. Microstructure analysis revealed primarily columnar austenite dendrites and δ-ferrite in an austenitic matrix, with grain shape influenced by deposition method and thermal history. Similarly, Jain et al.**[2]** showed that CMT-assisted WAAM 316L stainless steel can be fabricated with homogeneous fusion and without major macroscopic defects, producing tensile properties comparable to wrought 316L stainless steel. The 316L stainless steel printed by WAAM-CMT has UTS and YS values of 592.31 MPa and 276.46 MPa, respectively, compared to 557.62 MPa and 284.39 MPa for wrought 316L steel. The elongation for 316L stainless steel printed by WAAM-CMT is 53.2%, and for wrought 316L stainless steel, it is 59.85%. Also, Wang et al. **[21]** examined the microstructural features and tensile properties of 316L stainless steel produced by the CMT-WAAM process. The as-built 316L showed multilayered microstructures with RA regions having finer grains and higher strength/elongation than OA regions. Transverse

elongation exceeded build-direction values, and microhardness varied in RA but was uniform in OA.

During WAAM deposition, repeated heating and cooling cycles cause complex solidification behavior and microstructural variation along the build height. WAAM-CMT 316L stainless steel typically consists of γ-austenite and residual δ-ferrite, with ferrite morphologies (skeletal, lathy, vermicular, globular, or acicular) varying according to local thermal conditions **[2, 3, 22]**. Lone et al. **[14]** reported that bottom, middle, and top regions exhibit different microstructural features and mechanical properties due to heat accumulation and reheating effects. YS and UTS decrease from bottom (387 ± 1.98 MPa and 590 ± 3.18 MPa) to top (370 ± 4.96 MPa and 587 ± 3.12 MPa), while elongation increases from 56.9% to 61.5% **[14]**. Although WAAM-CMT produces mechanically sound 316L parts, challenges such as local heterogeneity, residual stress, and anisotropy remain.

The mechanical properties of WAAM-CMT 316L strongly depend on process optimization. Jain et al. **[3]** showed that current, welding speed, and contact tip-to-work distance significantly influence UTS, microhardness, and residual stress. Jain et al. **[15]** further reported 16.56% higher UTS than wrought 316L with comparable elongation (86.2% vs. 87.5%). Other studies indicate maximum tensile strength of 590 MPa and average YS of 302 MPa, outperforming or matching cold-rolled plate **[17]**. Therefore, careful control of deposition parameters and post-processing is essential for reliable performance.

The mechanical response of WAAM-CMT 316L stainless steel has also been shown to depend strongly on process optimization. Jain et al. **[3]** reported that current, welding speed, and contact tip-to-work distance influence ultimate tensile strength, microhardness, and residual stress, with optimized parameters improving the balance between strength and residual-stress control. Jain et al. **[15]** also confirmed that WAAM 316L steel had a 16.56% higher UTS than wrought 316L steel; but they exhibited comparable values for elongation percentages of 86.2% and 87.5%, respectively. Other studies conclude that WAAM has a maximum tensile strength of 590 MPa, with an average yield strength of 302 MPa, which is higher than the tensile strength of cold rolled (CR) plate (557 MPa), while WAAM tensile strength is comparable to that of CR plate (305 MPa) **[17]**. Therefore, controlling both the deposition parameters and post-processing condition is important for improving the final performance of WAAM-CMT 316L components.

Post-treatments such as heat treatment, shot peening, or Friction Stir Processing (FSP) are widely applied to refine the microstructure, introduce compressive residual stresses, and improve the mechanical performance of WAAM-fabricated components against fatigue cracking and stress corrosion. Xu et al.**[22]** reported that in-situ rolling combined with heat treatment significantly refined the grain structure and improved both strength and ductility of WAAM 316L stainless steel. Rodrigues et al. **[23]** investigated the development and characterization of 316L SS /Inconel

625 functionally graded material fabricated by WAAM. Direct-interface 316L/Inconel 625 FGMs showed higher strength (542 MPa), greater ductility (61.6%), and lower residual stress (≤180 MPa) than smooth-transition FGMs, which formed secondary phases and exhibited higher residual stresses. In addition the mechanical behavior of multi-layer SS 316L structures fabricated through GMAW-based WAAM was examined by Vora et al. **[24]**. confirmed that GMAW-based WAAM 316L exhibits position-dependent microstructural gradients along the build height, with mechanical properties comparable to wrought counterparts. The effect of laser shock peening intensity and its impact on the mechanical behavior of WAAM-fabricated SS316L was investigated by Thangamaniet al**. [25]**. The LSP induced severe surface plastic deformation, formed an oxide layer, and reduced porosity from 14.02 % to 4.18 %. The other part, LSP increased tensile strength and ductility (from 548 MPa/56.5 % to 634.5 MPa/59.7 %) via grain refinement and compressive residual stresses.

Among these strategies, shot peening stands out for its industrial simplicity and its ability to selectively strengthen the near-surface region without modifying the bulk material chemistry, which represents a key advantage over thermal post-treatments. This makes it particularly well-suited to address the surface anisotropy and mechanical heterogeneity that are inherent to the WAAM-CMT deposition process. Studies on additively manufactured 316L stainless steel have shown that shot peening and related surface post-processing treatments can improve surface integrity and residual-stress state, while the main microstructural changes remain concentrated near the surface rather than throughout the bulk material **[22-24, 26, 27]**.

Previous studies have thoroughly described the two-phase (γ-austenite/δ-ferrite) microstructure and the good strength-ductility combination of WAAM-CMT 316L stainless steel. However, important gaps remain: most works focus on deposition parameters (current, travel speed, trajectory) while giving limited attention to the complex thermomechanical effects from repeated heating-cooling cycles. Additionally, although post-treatments like shot peening can improve microstructure and properties, few studies have examined their combined interaction with process parameters. Internal defects (porosity, microcracks) and mechanical anisotropy also continue to challenge part reliability. This study addresses these gaps by systematically investigating the coupled effects of deposition parameters and shot peening on the microstructure and mechanical properties of 316L stainless steel produced by CMT-WAAM. Particular attention is given to the influence of build position (bottom, middle, top), with the aim of identifying optimal parameters for enhanced mechanical performance and surface quality in advanced engineering applications.

2. Materials and methods

2.1. Materials

Because of its excellent corrosion resistance and good weldability, the 1 mm diameter AISI 316L stainless steel wire was selected for the present research work. The chemical composition of the wire is detailed in Table 1.

Table 1. Chemical compositions of the SS 316L wire (wt. %).

Elements	C	Cr	Ni	Mo	Mn	Si	S	P	Fe
wt. %	0.013	19.24	12.92	2.64	1.68	0.30	0.0021	0.020	Bal.

2.2. WAAM setup and process parameters

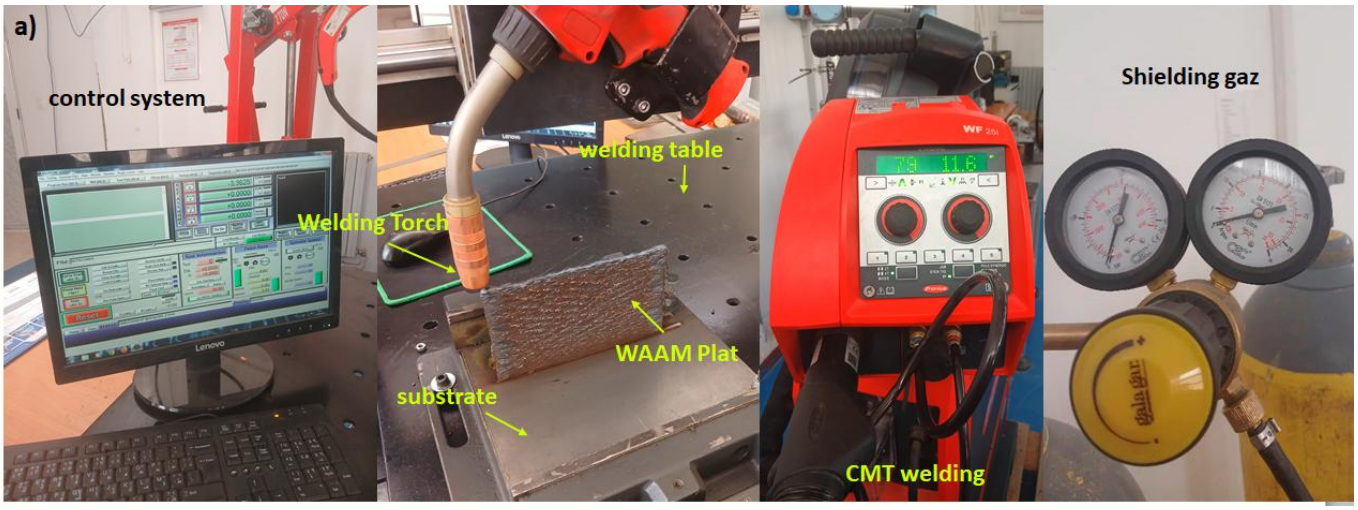
In the present study, the WAAM process was employed to fabricate metallic plates using a Fronius TPS 500i Cold Metal Transfer (CMT) welding system, as illustrated in Figure 1. The additive manufacturing operations were carried out using the 12 CrNi 199 ER 308 welding program, in combination with a shielding gas composed of 92% argon and 8% carbon dioxide, ensuring adequate arc stability and protection of the molten pool. During the deposition, the substrate plate was fixed to the worktable and a printing torch was moved along the two axes (x, z) to deposit the material onto the plate as illustrated in figure 1(b).

The process parameters were carefully optimized to ensure dimensional accuracy and structural integrity as illustrated in Table 2. The key parameters included a material thickness of 1.0 mm, a wire feed rate of 3.8 m/min, a welding current of 75 A, a voltage of 11.1 V, and a travel speed of 0.74 m/min. These settings were selected based on preliminary trials to balance heat input, deposition rate, and surface quality. The printing process was conducted such that each new layer was initiated precisely at the endpoint of the preceding one, ensuring continuity and consistent deposition. The resulting walls measured 170 mm in length and 100 mm in width and were built upon a substrate with a thickness of 20 mm, providing sufficient mechanical support and thermal mass during fabrication.

Table 2. Process parameters and their values.

Parameters	**Unit**	**Value**
Welding mode	-	MAG CMT
Current	A	75
Voltage	V	11.1
Travel speed	mm/min	700
Wire feed rate	mm/min	3.8
Shielding gas	-	Argon + CO_2
Filler wire diameter	mm	1.0

Torch angle	degree	90°
Gas flow	l/min	15



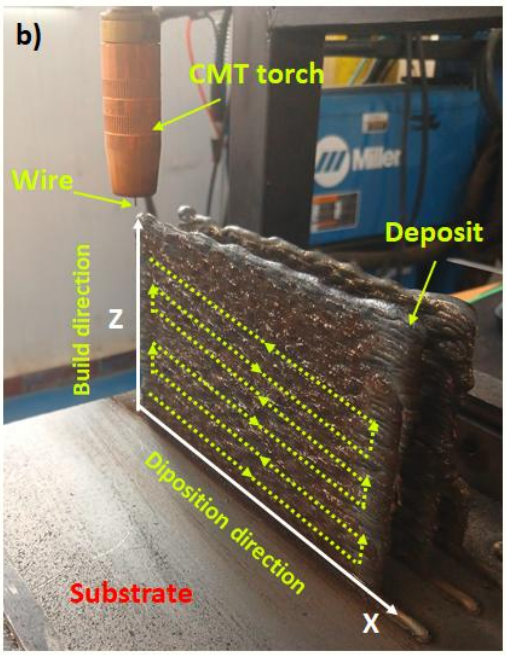


Figure 1. a) Experimental setup of the WAAM process using Cold Metal Transfer technology, b) representative example of a part manufactured and WAAM deposition process.

2.3. Shot peening setup and conditions WAAM Deposition Direction

Following the WAAM fabrication, shot peening was applied as a post-processing step to enhance the surface integrity and mechanical performance of the printed components. This

treatment was performed using an ALFA 20 rotary table shot peening machine manufactured by Turbotecnica (Italy), as illustrated in Figure 2. The machine features a rotary table with a diameter of 2000 mm and a vertical clearance of 2000 mm, allowing for the treatment of components with diameters ranging from 40 mm to 420 mm and lengths up to 1000 mm. The system supports a maximum workpiece weight of 30 kg, with an overall load capacity of 1000 kg, making it suitable for both individual parts and batch processing. It is equipped with two high-performance turbines, each delivering 75 kW of power, and capable of operating at a shot flow rate of 220 kg/min.

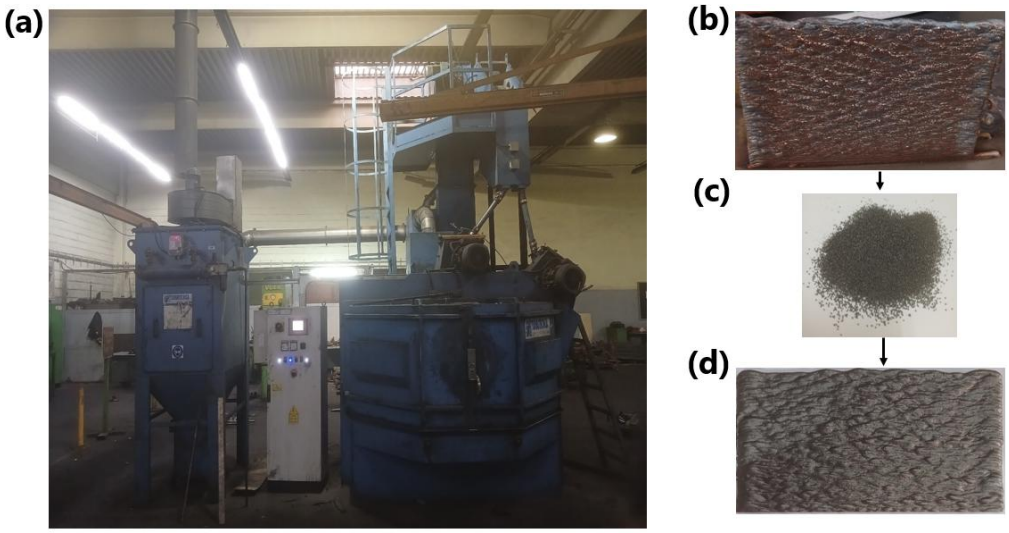


Figure 2. (a) Shot peening machine setup (ETRAG Constantine Algeria); (b) WAAM-fabricated sample in the as-built condition; (c) spherical steel shot media (Ø 0.5 mm); (d) WAAM sample after shot peening treatment.

For the current study, the turbines were adjusted to a rotational speed of 1000 rpm to ensure uniform and consistent peening across the surface of the printed specimens. The shot peening operation was conducted over a duration of 15 minutes, using spherical steel media with a diameter of 0.5 mm (Figure2(c)). This configuration was chosen to induce beneficial compressive residual stresses on the surface while minimizing surface damage, thereby improving fatigue resistance and overall mechanical performance. Figure 2(d) shows the surface of the plate after shot peening.

2.4. Mechanical tests

To evaluate the mechanical behavior of the structures manufactured using the WAAM process, horizontal tensile specimens were extracted from the central region of the printed walls at three different heights: bottom, middle, and top (Figure 3(b)). Specimens were taken from the most homogeneous zone of the walls in order to avoid typical defects occurring at the beginning and end of the deposition process. Figure 3(c) provides a detailed illustration of the vertical location of specimen extraction within the printed wall, as well as the specimen geometry in compliance with the aforementioned standard. To ensure the reproducibility of the mechanical

tests and compliance with standard requirements, the specimen geometry was rigorously defined in accordance with the ASTM B557M-06 standard (Figure 3(d)), which specifies the procedures for the preparation and tensile testing of metallic materials, using a servo-hydraulic MTS Criterion universal testing machine, Model 45 with a maximum load capacity of 100 kN.

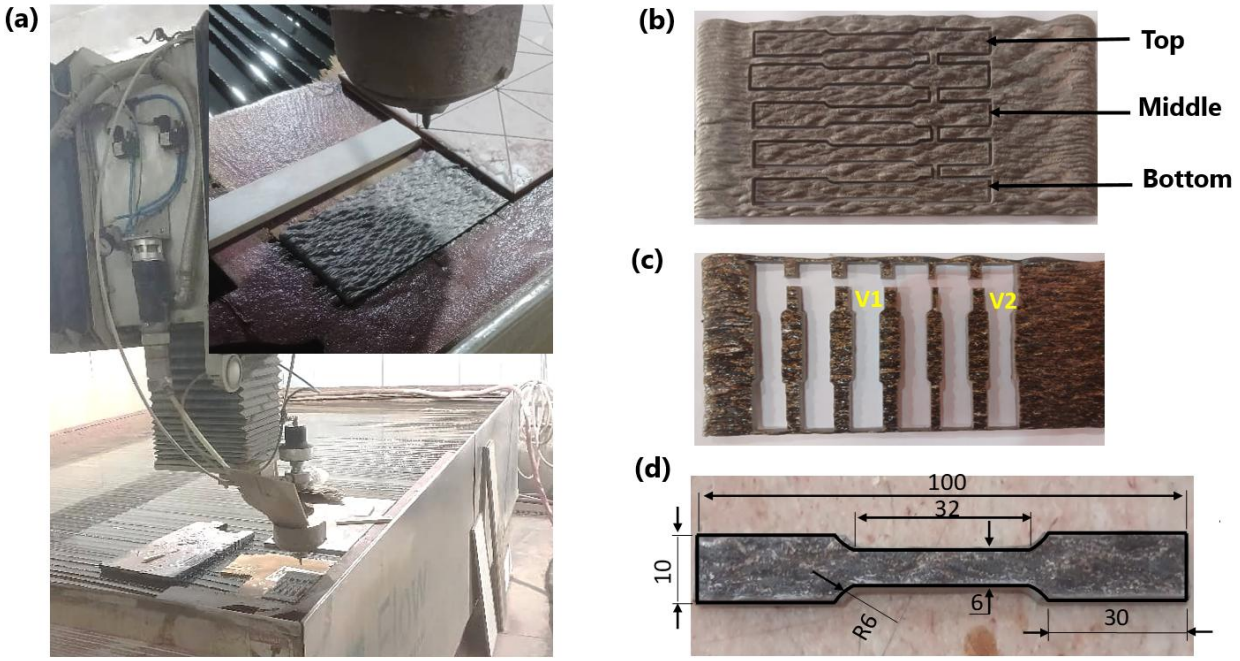


Figure 3. (a) Water jet cutting table, (b) WAAM sample cut by water jet horizontally, (c) WAAM sample cut by water jet vertically, and (d) sample dimensions.

A quasi-static strain rate of 0.05 mm/s was applied to obtain accurate stress–strain curves, enabling characterization of both the elastic and plastic behavior of the material. For each set of processing conditions, three specimens were tested to ensure result reproducibility and meaningful statistical analysis.

Alongside tensile tests, microhardness measurements were conducted to assess the local mechanical response across the deposited walls. The microhardness was measured at three distinct positions of the wall (bottom, middle, and top) along both horizontal and vertical directions. Indentation spacing was set to 2 mm for horizontal measurements and 1 mm for vertical measurements, using a test load of 0.5 HV.

2.5. Microstructural characterization

The microstructural characteristics of the samples, in both the as-built condition and after post-processing (shot peening), were examined using optical microscopy, providing valuable insights into grain morphology, phase distribution, and potential defects (such as porosity, lack of

fusion, etc.). These observations are essential to understand the influence of processing parameters and surface treatments on the final properties of WAAM-fabricated components. For microstructural characterization, the samples were sequentially ground using 80, 120, 240, 600, 800, and 1200 grit abrasive papers. Final polishing was carried out on felt paper. Following polishing, the samples were chemically etched using V2A reactant, composed of 100 ml hydrochloric acid (37% HCl) and 10 ml nitric acid (69% HNO_3), with an etching duration of approximately 5 to 6 minutes. The microstructure of the material surface was then analyzed using an Olympus DSX-1000 optical microscope.

2.6. SEM-EDX fractography

The fracture surfaces of the tensile-tested WAAM 316L stainless steel specimens were examined using a QUANTA FEG 250 scanning electron microscope (SEM) to understand and compare the fracture behavior of as-built and shot-peened conditions.

3. Results and discussion

The influence of shot peening on the microstructural and mechanical properties of 316L stainless steel produced by WAAM-CMT are examined. Specimens were taken from different regions of the wall (bottom, middle, and top) in both as-processed and shot-peened conditions to evaluate the evolution of tensile behavior, microhardness, and microstructure. The main objective is to determine the extent to which shot peening can improve the mechanical and microstructural uniformity of the material along the construction height and thus optimize the overall performance of WAAM-CMT-manufactured parts.

3.1. Tensile properties

Figure 4 shows the tensile stress–strain curves of SS 316L specimens produced via the WAAM-CMT process, for both as-built and shot-peened conditions, extracted from the bottom, middle, and top regions of the deposited wall. Specimens were prepared in the horizontal direction relative to the deposition orientation.

Figure 4(a) shows the stress–strain responses of the as-built specimens, highlighting the variations in tensile behavior among samples taken from different wall heights, which reflect the effect of process-induced thermal gradients and microstructural heterogeneity along the build direction. In the initial slope (elastic region), all three curves overlap closely, indicating a similar elastic modulus regardless of build height. The yield strength (YS) is highest in the bottom region and have slightly lower values in the middle region. The ultimate tensile strength (UTS) is highest (~480 MPa) in the bottom region, and a value of around (~420 MPa) in the middle and top regions. The ductility (strain at fracture) is less in the bottom region (~32 %), and higher in the middle and top regions (~40 %). The lower ductility in the bottom region results from rapid cooling because of contact with the cold substrate plate early in the build, producing finer grains and residual

compressive stresses that raise strength, and possible differences in microstructure (e.g., more ferrite or refined austenite) from thermal gradients. The top and middle regions of the part exhibit slightly lower strength but greater elongation due to slightly coarser grains and lower residual stresses. In summary, the bottom region exhibits higher strength and lower ductility, whereas the middle and top regions show lower strength and higher ductility.

Figure 4(b) presents the tensile stress-strain curves of the shot-peened specimens. In the elastic region, the curves almost coincide, indicating that the elastic modulus is not affected by shot peening and by the specimen location. For all the zones (bottom, middle and top), the yield strength (YS) is slightly higher than their as-built counterparts, while a minimal difference is observed between the shot-peened specimens taken from the bottom, middle, and top locations. In contrast, the Ultimate Tensile Strength (UTS) values cluster around ~470 - 511 MPa, being slightly higher than those of the as-built middle and top regions and comparable to the as-built bottom region. In addition, ductility (elongation) decreases to approximately 25 - 27% across all regions, which is significantly lower than that of the as-built samples, particularly in the middle and top regions, where the reduction in elongation for shot-peened specimens reaches approximately 45%. The shot peening process introduces surface cold work and compressive residual stresses, which induce work hardening and grain refinement near the surface, raising yield strength (YS) and slightly increasing UTS, and reduce overall ductility because the hardened surface limits plastic deformation and promotes earlier crack initiation.

Overall, for the as-built case, the bottom region shows the highest yield strength, while the middle and top have slightly lower yield values. Elongation to fracture is greatest in the middle and top, around 40 %, and somewhat lower at the bottom, about 32 %. After shot peening, the mechanical properties become uniform across all regions. The yield strength (YS) increases slightly and is nearly the same for all the regions (bottom, middle, and top). The ultimate tensile strength (UTS) falls within a narrow range of about 470–490 MPa for all zones, essentially matching the former bottom value. However, the elongation decreases for every region, settling at roughly 25 %, showing little difference from top to bottom regions.

A clear difference was observed in the tensile curves of as-built specimens extracted from the bottom, middle, and top regions of the fabricated wall. In contrast, specimens from the shot-peened wall displayed nearly overlapping curves for all the three locations. This uniformity highlights the strong influence of shot peening on the mechanical behavior of the WAAM-CMT fabricated 316L stainless steel material. The process introduces compressive residual stresses that effectively counteract the tensile residual stresses generated during additive manufacturing, leading to a more homogeneous stress state and consistent tensile response across the entire wall. In short, shot peening raises strength across the wall height while reducing total elongation

compared to the as-built samples, demonstrating the process's strengthening on the WAAM-CMT 316L stainless steel.

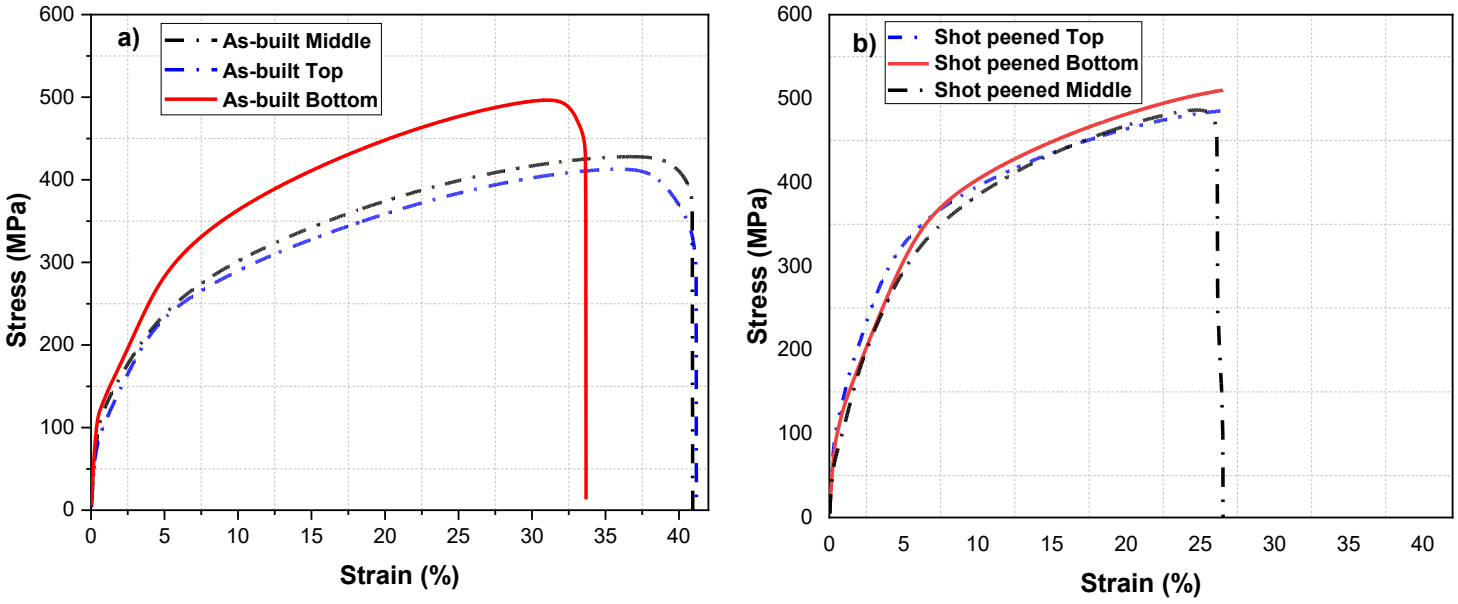


Figure 4. Tensile curves of SS 316L WAAM-CMT specimens cut horizontally (as-built and shot-peened) taken from the bottom, middle, and top regions of the wall.

Figure 5 shows the results of tensile tests carried out on specimens cut vertically along the printing line. These specimens were taken from the center of the wall (V1) and from the side of the wall (V2), and were analyzed both in their initial state and after mechanical treatment by shot peening, thus allowing the influence of the manufacturing method and the treatment on the mechanical properties of the materials to be evaluated. The results show that the tensile strength of samples taken from the center (V1) is consistently higher than that of samples taken from the side (V2), both in the initial and shot-peened states. This difference could be related to the effects of additive manufacturing, which can create gradients in mechanical properties within the part.

Shot peening resulted in a significant improvement in tensile strength. In particular, sample V1 showed an increase in tensile strength, reaching 514.26 MPa after shot peening, representing a 10% improvement over the initial state, suggesting material strengthening through the induction of compressive residual stresses at the surface. Data from Figures 5(a) and (b) indicate that, for both samples, the ultimate tensile strength (UTS) increases after shot peening, but with a

concomitant reduction in strain. For sample V1, the tensile strength increases from 468.08 MPa to 514.26 MPa, while the strain decreases from 32.12% to 26.55%. For sample V2, the tensile strength increases from 358.59 MPa to 467.91 MPa, and the strain decreases from 31.16% to 22.07%. This reduction in deformation after shot peening can be interpreted as a surface hardening of the material, which improves strength but reduces ductility. Consequently, the results show that the WAAM-CMT method combined with shot peening improves the tensile strength of the materials, but this improvement is accompanied by a reduction in ductility. The sample taken from the center of the wall (V1) exhibits better mechanical performance than the one taken from the side (V2), suggesting that the geometry of the part and the property gradients influence the results of the tensile tests.

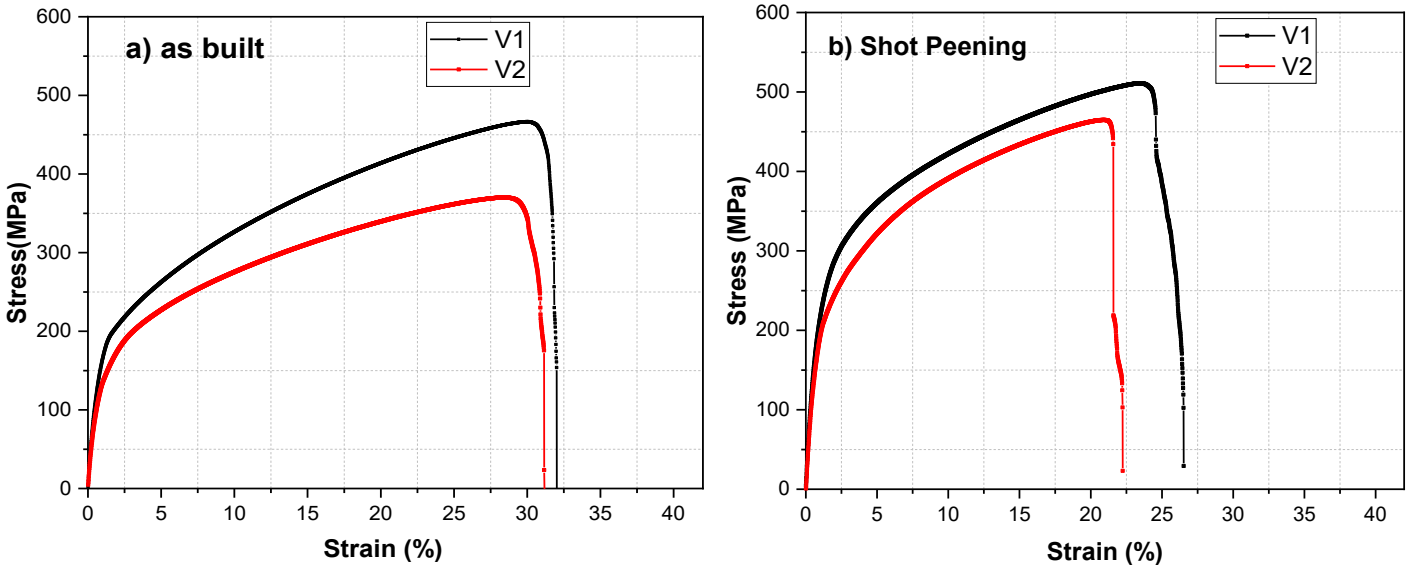


Figure 5. Tensile stress-strain curves of SS 316L WAAM-CMT specimens cut vertically (as-built and shot-peened), taken from the left and middle of the wall.

A similar trend was reported by Thangamani et al.**[25]** who found that laser shock peening increased the UTS of WAAM SS316L from 548 MPa to 595–634.5 MPa, with a maximum improvement of 15.8%. In WAAM carbon steel treated by severe shot peening, Hietala et al.**[28]** also reported an increase in UTS by 2.5%, reaching a peak tensile strength of 513 MPa, together with improved surface hardness and fatigue resistance. These studies support the present result that peening-based surface treatment can improve tensile strength in WAAM materials, although the main strengthening effect remains concentrated near the surface.

3.2. Microstructural characterization

In general, the microstructure of 316L stainless steel parts manufactured by WAAM-CMT depends on several parameters, including their position within the part, heat treatments, cooling rate, and mechanical treatments such as shot peening or cold rolling. These factors influence not only the mechanical strength but also the ductility and surface properties of the material. In this work, the microstructure of 316L stainless steel walls produced by WAAM-CMT process was studied before and after shot peening using cross-sections (Figure 3). The analysis was conducted on three distinct zones of the wall: top zone, middle zone, and bottom zone. Before any mechanical treatment, the microstructure of the 316L stainless steel walls obtained by WAAM-CMT consists mainly of austenite (γ) dendrites and residual δ ferrite, distributed within a predominantly austenitic matrix (Figures 6–8).

Furthermore, the microstructure varies significantly depending on the position within the part. In the bottom zone of the wall, fine equiaxed grains are observed, associated with globular and skeletal δ-ferrite. The middle zone is characterized by fine, columnar grains containing predominantly skeletal and vermicular δ-ferrite. In contrast, the top zone exhibits coarser columnar grains, accompanied by acicular and lathy δ-ferrite **[5]**. This two-phase microstructure, composed of γ-austenite and δ-ferrite, with skeletal and lathy morphologies, is comparable to that observed in conventional rolled 316L stainless steel **[2]**.

For the as built case from the middle zone (Figure 6 (a)), the microstructure exhibits features typical of WAAM-produced austenitic stainless steels. Elongated columnar grains are observed, preferentially oriented along the heat flow and deposition direction. This grain morphology is mainly attributed to the high thermal gradients and directional solidification inherent to the WAAM-CMT process. The microstructure shows noticeable grain size homogeneity, with the presence of coarse grains extending across multiple deposited layers. At the sub-grain scale, a cellular or dendritic structure is generally present, resulting from repeated thermal cycling. Such a microstructural anisotropy is known to influence the mechanical response, particularly in terms of directional dependence of strength and fatigue behavior.

Following shot peening (Figure 6(b)), significant microstructural modifications are observed, especially near the surface. The treated region exhibits a pronounced grain refinement compared to the as-built condition. This refinement is induced by severe plastic deformation generated by the repeated impacts of the shot particles. Shot peening introduces a high density of dislocations and promotes the formation of refined grains, leading to a more homogeneous microstructure in the affected surface layer. In addition, the initial columnar grain morphology becomes less pronounced, indicating a partial suppression of microstructural anisotropy at the surface. The induced compressive residual stresses and refined grain structure are expected to

enhance surface-related properties, including hardness and fatigue resistance, by delaying crack initiation and propagation.

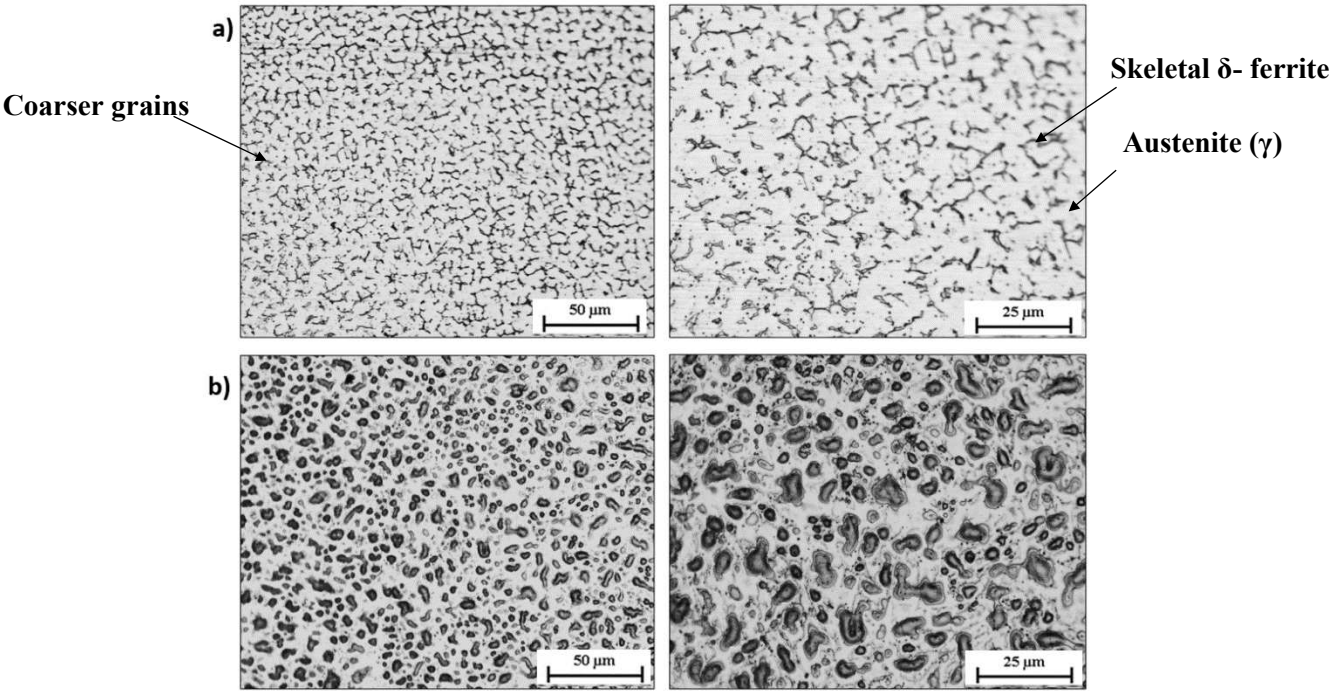


Figure 6. Microstructure of WAAM-CMT-fabricated SS 316L in the middle wall zone: (a) as-built, and (b) shot peened.

In the bottom zone, the as-built case (Figure 7(a)) exhibits a microstructure characterized predominantly by elongated columnar grains, aligned along the build direction. Due to its proximity to the substrate, this region experiences higher heat dissipation, resulting in a relatively finer grain structure because of rapid solidification compared to the middle and upper wall regions (Figures 6 and 8). The repeated thermal cycles, higher thermal gradients and rapid cooling promote directional solidification, leading to microstructural anisotropy. Cellular or dendritic substructures are typically observed within the grains, originating from rapid solidification and solute redistribution during the WAAM-CMT process. Although the grain size is comparatively refined.

After shot peening (Figure 7(b)), pronounced microstructural refinement is observed in the near-surface region of the bottom zone. The impact-induced plastic deformation leads to the fragmentation of the initial grains and the formation of refined grains with a more equiaxed morphology. The columnar grain orientation is significantly disrupted in the peened layer, indicating a reduction in microstructural anisotropy at the surface. The high density of dislocations introduced by shot peening contributes to grain subdivision and enhances strain hardening effects

and mechanical properties. These microstructural modifications are associated with the compressive residual stresses, which are beneficial for improving surface hardness and resistance to fatigue crack initiation, particularly critical in the bottom region where load transfer to the substrate is significant. Compared to the middle region, the bottom zone exhibits inherently finer grains in the as-built condition due to higher cooling rates near the substrate. However, shot peening remains effective in both regions, producing consistent grain refinement and microstructural homogenization at the surface. This indicates that shot peening is a robust post-processing technique capable of mitigating microstructural anisotropy across different build heights in WAAM-CMT SS 316L components.

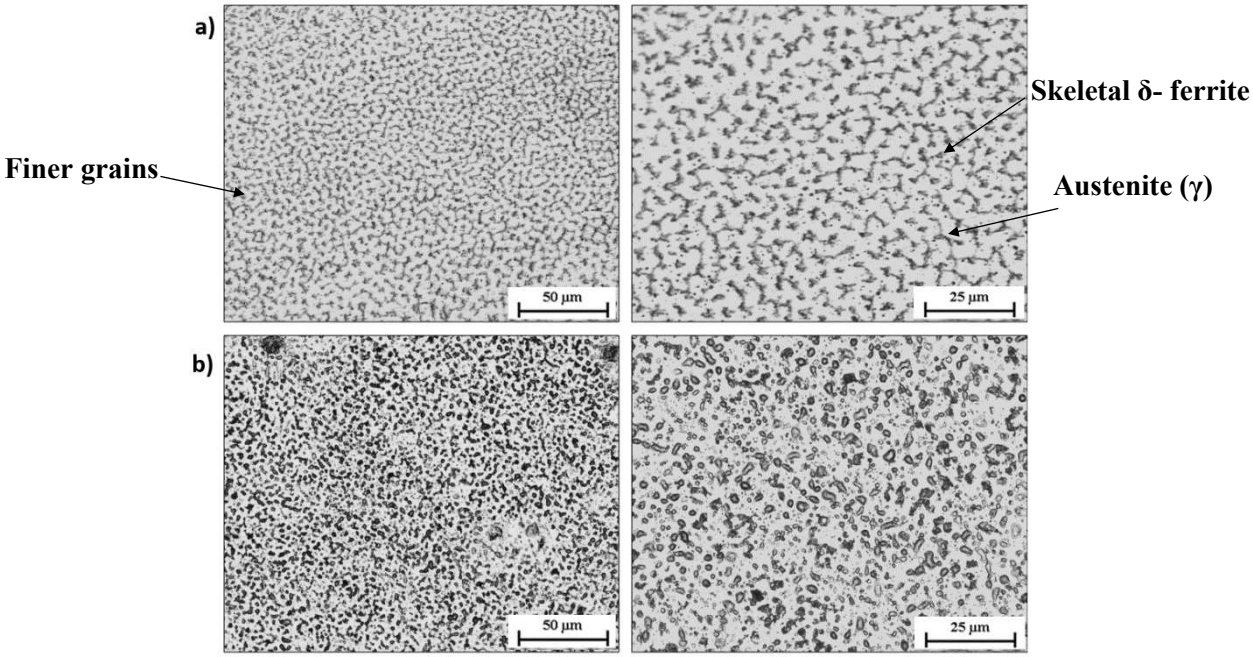


Figure 7. Microstructure of WAAM-CMT fabricated SS 316L in the bottom area: (a) as-built, and (b) shot peened.

In the top zone, the as-built state (Figure 8(a)) exhibits a microstructure dominated by coarse columnar grains with a pronounced preferential orientation along the build direction. Compared to the bottom and middle regions, the grains in the top wall are noticeably larger, which can be attributed to lower heat dissipation and reduced cooling rates at higher build heights. The accumulation of thermal cycles and prolonged exposure to elevated temperatures promote grain growth and coarsening. As a result, a higher degree of microstructural anisotropy is observed in this region. Cellular or dendritic substructures within the grains are typically present, reflecting the solidification conditions inherent to the WAAM-CMT process. Such coarse and oriented grain structures may negatively affect mechanical properties, particularly fatigue resistance and isotropic behavior.

After shot peening (Figure 8(b)), substantial microstructural refinement is observed in the near-surface region of the top wall. The severe plastic deformation induced by the peening impacts leads to the subdivision of the initial coarse grains and the formation of refined, more equiaxed grains. The treatment significantly reduces the apparent columnar grain morphology at the surface, resulting in a more homogeneous microstructure. A high density of dislocations is introduced, contributing to strain hardening and the development of compressive residual stresses. Despite the initially coarse as-built microstructure in the top wall, shot peening proves effective in modifying the surface layer, thereby enhancing surface integrity and mitigating the detrimental effects associated with grain coarsening.

A clear microstructural gradient is observed along the wall height in the as-built condition, with grain size increasing from the bottom to the top wall. This gradient reflects the variation in thermal history during the WAAM-CMT process. However, shot peening consistently induces grain refinement and microstructural homogenization in all regions, regardless of their initial grain size. This demonstrates that shot peening is an effective post-processing technique for reducing surface anisotropy and improving the overall performance of WAAM-CMT SS 316L components.

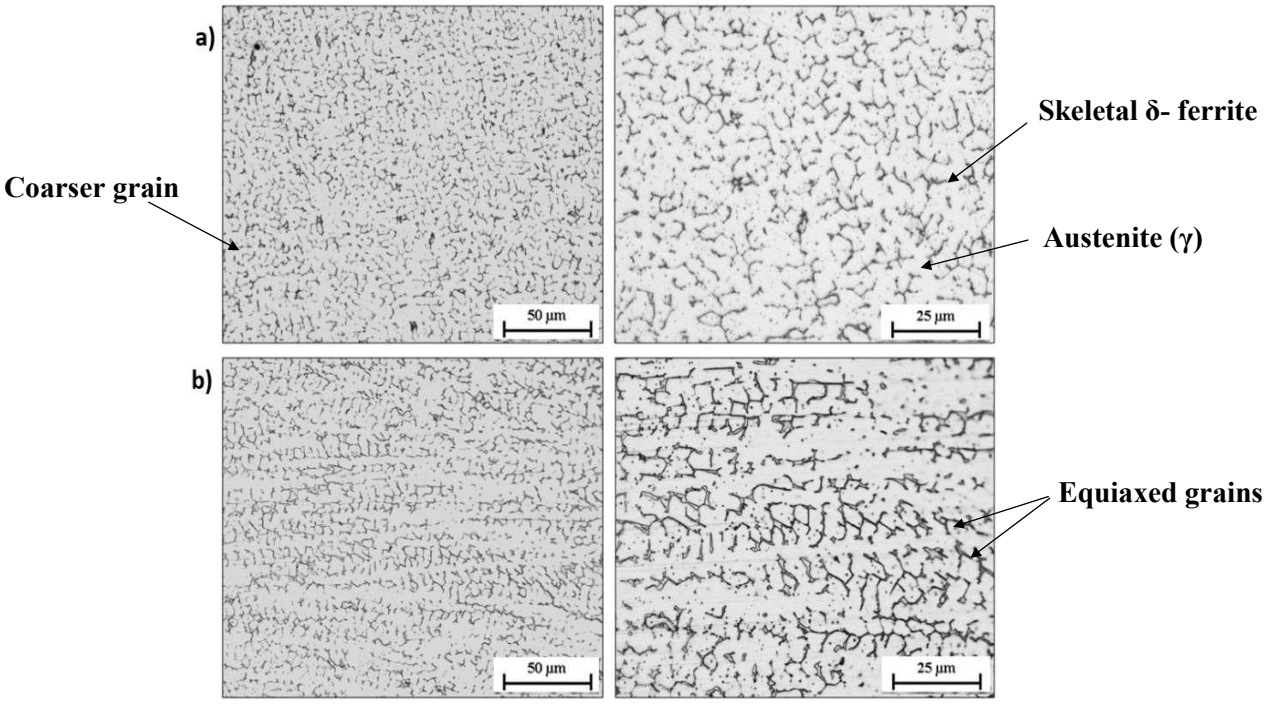


Figure 8. Microstructure of WAAM-CMT fabricated SS 316L in the top area: (a) as-built, and (b) shot peened.

Figure 9 presents the evolution of grain size in WAAM-CMT fabricated SS 316L, comparing the as-built and shot-peened conditions at three different zone of wall (bottom, middle, and top).

Shot peening significantly modifies the grain structure across the wall height, although the magnitude and nature of the effect depend on both the local microstructure and phase distribution.

In the bottom region, the ferritic phase exhibits a pronounced grain refinement, with the mean grain size decreasing from 14.346 μm in the as-built condition to 5.342 μm after shot peening. This refinement is associated with severe plastic deformation induced by the high-velocity impacts, which generate a high density of dislocations. These dislocations rearrange into sub grain structures and progressively transform into high-angle grain boundaries through continuous dynamic recrystallization (CDRX). As a result, a nanostructured ferritic surface layer is formed, leading to improved hardness, strength, and fatigue resistance. Similarly, the pearlite-like phase shows a reduction in mean grain size from 16.111 μm to 8.814 μm after shot peening. The lamellar ferrite carbide colonies are fragmented by plastic deformation, producing an ultrafine ferritic matrix with finely dispersed carbides.

In the middle region of the wall, the response to shot peening is more complex. The ferritic phase shows an apparent increase in mean grain size from 5.263 μm to 14.824 μm after treatment. Although shot peening generally promotes grain refinement, localized thermal spikes, strain gradients, and dynamic recovery may activate static or dynamic recrystallization mechanisms, leading to abnormal grain growth in selected regions. This behavior can occur when stored strain energy is unevenly distributed and grain boundary mobility locally exceeds pinning forces. In contrast, the pearlite-like phase in the middle region undergoes substantial refinement, with grain size decreasing from 13.221 μm to 4.801 μm, confirming the dominant role of severe plastic deformation and CDRX in breaking down lamellar structures.

At the top of the wall, the ferritic phase exhibits nearly identical grain sizes before and after shot peening (2.347 μm and 2.478 μm, respectively). This indicates a balance between grain refinement and recovery mechanisms, where newly formed recrystallized grains grow only until equilibrium is reached between boundary energy and stored strain energy. Particle pinning effects further suppress abnormal grain growth, resulting in a stable and uniform grain size distribution. Conversely, the pearlite-like phase shows a slight grain coarsening after shot peening, increasing from 39.195 μm to 44.518 μm. Although grain refinement is generally expected, localized loss of carbide pinning, thermal effects, and strain heterogeneity during peening can promote abnormal grain growth in isolated regions. Such counter-intuitive behavior has been reported in heavily deformed multiphase steels under non-uniform deformation conditions.

Overall, shot peening reduces microstructural heterogeneity along the wall height and promotes grain refinement in most regions, particularly where coarse grains are present in the as-built condition. According to the Hall–Petch relationship, this refinement is expected to enhance mechanical performance. Despite localized grain coarsening in specific phases and regions, the global effect of shot peening is a more homogeneous and mechanically favorable microstructure, confirming its effectiveness as a post-processing technique for WAAM-CMT fabricated SS 316L components.

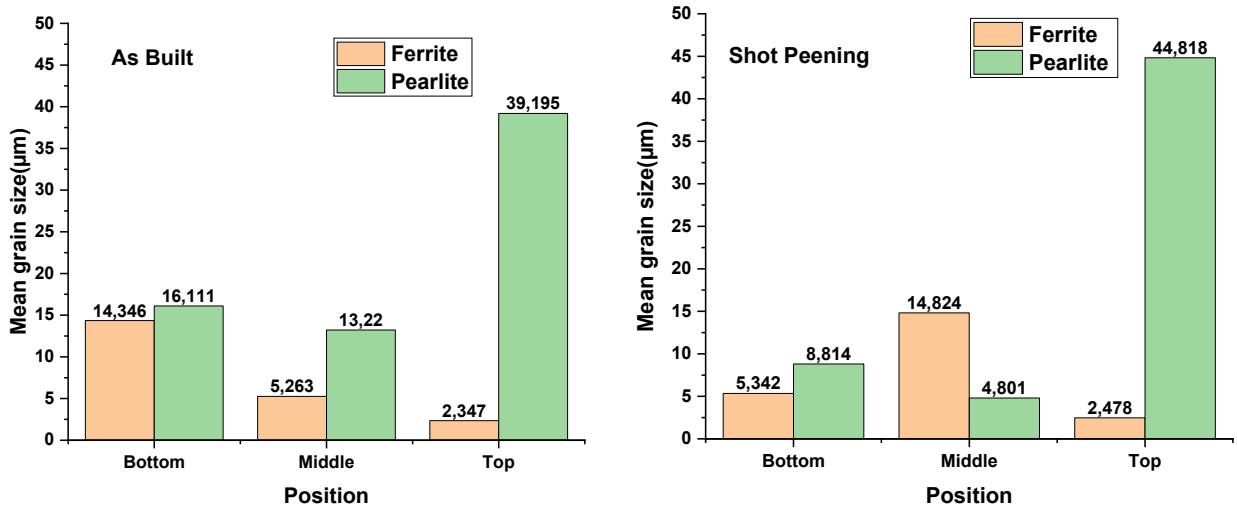


Figure 9. Grain size of as-built and shot peened SS 316L WAAM-CMT in different zones (bottom, middle, and top) of the wall.

3.3 Microhardness analysis

Figure 10 presents the Vickers microhardness of WAAM-CMT fabricated SS 316L in the as-built and shot-peened conditions, measured along the horizontal direction at three build heights (bottom, middle, and top). The hardness evolution is discussed in direct relation to the microstructural features described in the previous section.

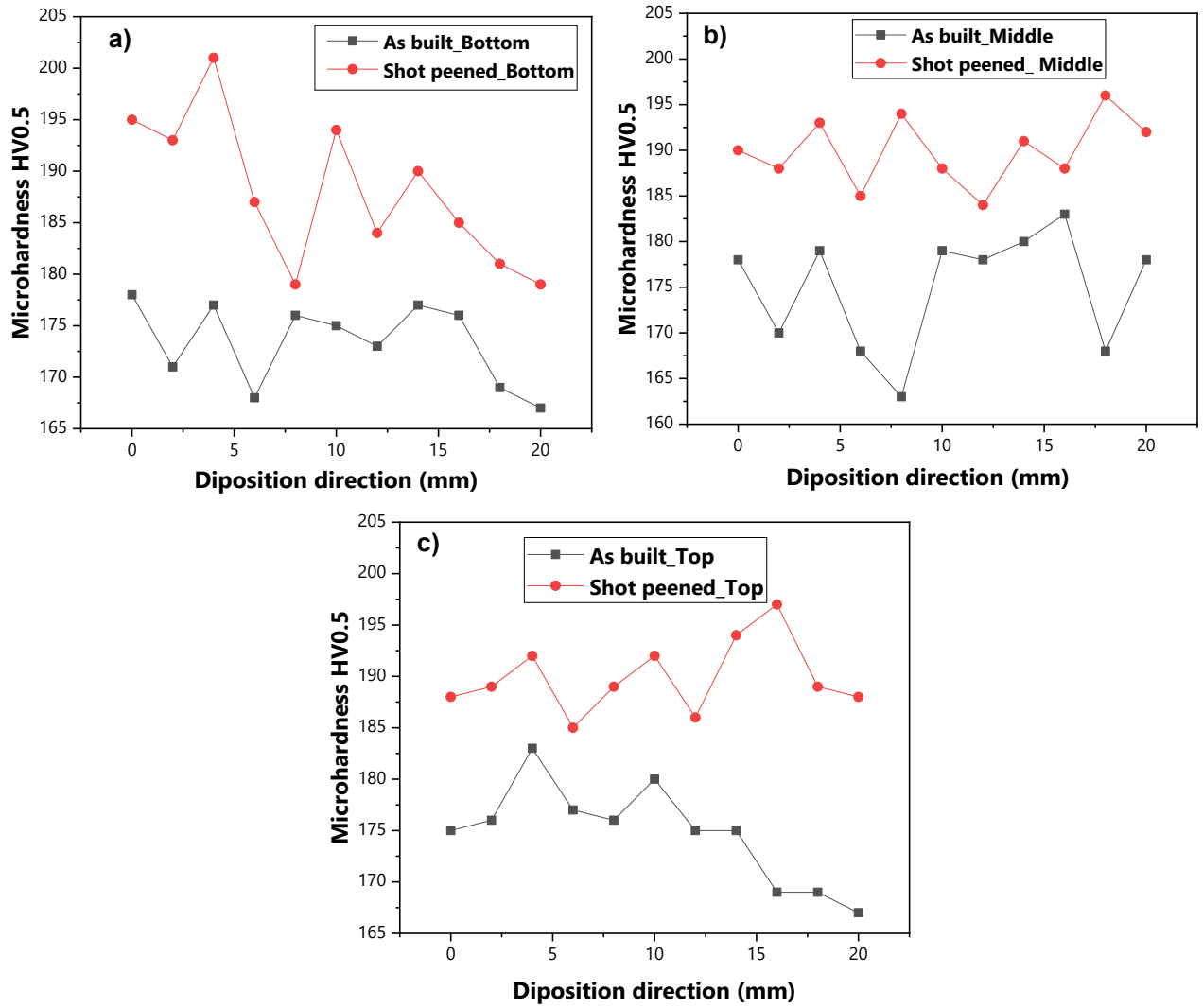
In the as-built state, a gradual decrease in microhardness is observed from the bottom to the top of the wall. Average hardness values of approximately 183.16 HV, 182.19 HV, and 177.83 HV are measured in the bottom, middle, and top regions, respectively. This hardness gradient is consistent with the grain size evolution along the build direction. The bottom region, which exhibits finer grains due to repeated thermal cycling and higher effective cooling rates, shows the highest hardness values. In contrast, the middle and top regions characterized by progressively coarser grains and reduced thermal cycling, display lower hardness. This behavior follows the Hall–Petch relationship, where by finer grain sizes enhance resistance to plastic deformation. The relatively smooth hardness gradient further indicates that, despite microstructural heterogeneity,

the WAAM-CMT process produces a mechanically stable build with a limited risk of localized brittle behavior. Shot peening leads to a marked increase in microhardness at all build positions, in agreement with the grain refinement observed in the microstructural analysis (Figure 9). In the bottom region, where the ferritic grain size is reduced from approximately 14.35 μm in the as-built condition to ~5.34 μm after shot peening, the microhardness increases to values exceeding 185–190 HV. This enhancement arises from the combined effects of severe plastic deformation, grain refinement through continuous dynamic recrystallization, and the introduction of compressive residual stresses.

In the middle region, although localized grain coarsening of the ferritic phase is observed after shot peening (from ~5.26 μm to ~14.82 μm), the overall microhardness still increases to values around 180–185 HV. This apparent discrepancy can be explained by the dominant contribution of the ultrafine-grained and strain-hardened surface layer to the indentation response. In addition, the strong refinement of the pearlite-like phase, with grain size decreasing from ~13.22 μm to ~4.80 μm, contributes significantly to the net hardness increase, outweighing the localized ferritic grain growth.

At the top of the wall, the ferritic grain size remains nearly unchanged after shot peening (~2.35 μm in the as-built condition and ~2.48 μm after treatment), reflecting a balance between recrystallization and recovery mechanisms. Nevertheless, microhardness still increases from approximately 177–178 HV in the as-built state to about 180–186 HV after shot peening. This confirms that hardness enhancement is not governed solely by average grain size, but also by increased dislocation density, subgrain formation, and compressive residual stresses induced by shot peening.

Figure 10. Distribution of microhardness in as-built and shot-peened SS 316L fabricated by



WAAM-CMT, measured horizontally along the deposition direction: (a) bottom, (b) middle, and (c) top.

Figure 11 illustrates the evolution of the average microhardness of 316L stainless steel in the as-built state and after shot peening, measured vertically along the height of the WAAM-CMT wall. Indentations were made at various positions (the bottom, the middle and the top) to assess the influence of microstructural gradients induced by the thermal cycles of the additive manufacturing process. In the as-built state, the results reveal a progressive variation in microhardness along the vertical direction. This heterogeneity is primarily attributed to repeated thermal cycles and heat accumulation at the base of the wall, which promote grain growth and a local reduction in dislocation density. Conversely, the upper regions, solidified under higher cooling rates, exhibit a finer microstructure, resulting in slightly different levels of microhardness.

After shot peening, a significant increase in microhardness is observed along the entire vertical direction. This behavior is linked to the plastic deformation induced at the surface, leading to work hardening, an increase in dislocation density, and the introduction of compressive residual stresses. Furthermore, the microhardness distribution becomes more homogeneous along the vertical axis, indicating that shot peening effectively mitigates the mechanical property gradients generated during WAAM manufacturing.

Overall, the evolution of microhardness closely follows the microstructural modifications induced by both the WAAM-CMT process and the shot peening treatment. While grain refinement plays a primary role in hardness enhancement, particularly in the bottom and middle regions, strain hardening and residual compressive stresses are equally critical in regions where grain size changes are limited or locally heterogeneous. Shot peening therefore acts as an effective post-processing technique that mitigates microstructural heterogeneity, reduces build-height-dependent mechanical gradients, and enhances the surface mechanical performance of WAAM-fabricated SS 316L components.

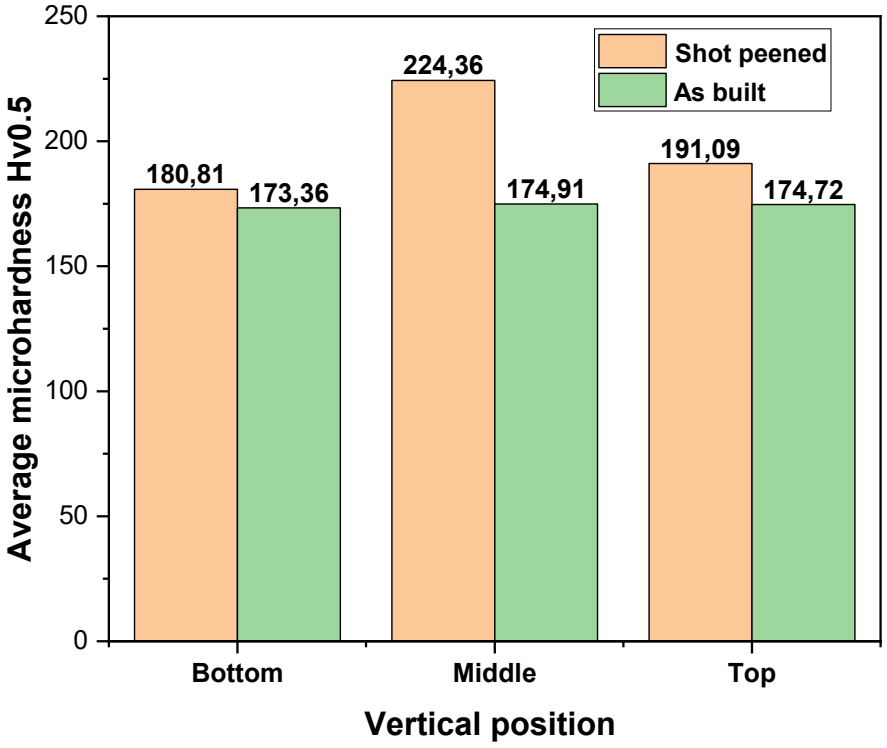


Figure 11. The average microhardness of as-built and shot-peened SS 316L fabricated by WAAM-CMT, measured vertically along the deposition direction: bottom, middle and top.

3.4. SEM-EDX fractography

SEM of the fracture surfaces of the tensile tested specimens are shown in Figure 12. These micrographs show a predominantly ductile fracture mode for both the as-built and shot-peened WAAM-CMT 316L stainless steel specimens. At low magnification, the as-built specimen (Figure 12(a)) shows an irregular fracture surface with a rough morphology, while the shot-peened specimen (Figure 12(e)) also exhibits a rough fracture profile but the fracture surface appears relatively less irregular. The higher-magnification images, Figures 12(b-d) and Figures. 12(f-h), show many dimples, which are typical features of ductile fracture caused by microvoid nucleation, growth, and coalescence. Similar dimple-dominated fracture morphologies have been reported for CMT-WAAM 316L stainless steel, where the presence of numerous dimples was associated with good ductility of the fabricated structure **[2]**.

For the as-built condition, the fracture surface shows fine and relatively uniformly distributed dimples, which indicates ductile fracture with homogeneous plastic deformation before final failure. This behavior is consistent with previous WAAM stainless-steel studies, where ductile fracture was linked to the austenitic matrix. WAAM 316L stainless steel commonly contains γ-austenite and δ-ferrite, including skeletal and lathy ferrite morphologies, which can influence void initiation and crack propagation during tensile loading**[2] [29]**.

After shot peening, the fracture surface still shows a ductile dimpled morphology, but the dimples appear deeper, locally coarser in some regions, and less uniformly distributed (Figures 12(g-h)), which may indicate localized microvoid growth before coalescence. The presence of ductile dimples after shot peening indicates that the WAAM-CMT 316L stainless steel retained its ability to deform plastically during tensile loading. However, the shot-peened specimen shows a more pronounced and coarser microvoid coalescence morphology, which may be related to the surface-hardened layer and residual-stress field introduced by the peening impacts. These effects can increase local resistance to plastic deformation and lead to strain localization, which contributes to the observed improvement in UTS, while also reducing elongation at failure, because part of the near-surface region has reduced capacity for further plastic deformation (due to prior plastic deformation during peening).

Overall, the SEM fractography confirms that both as-built and shot-peened WAAM-CMT 316L stainless steel specimens failed mainly by ductile microvoid coalescence.

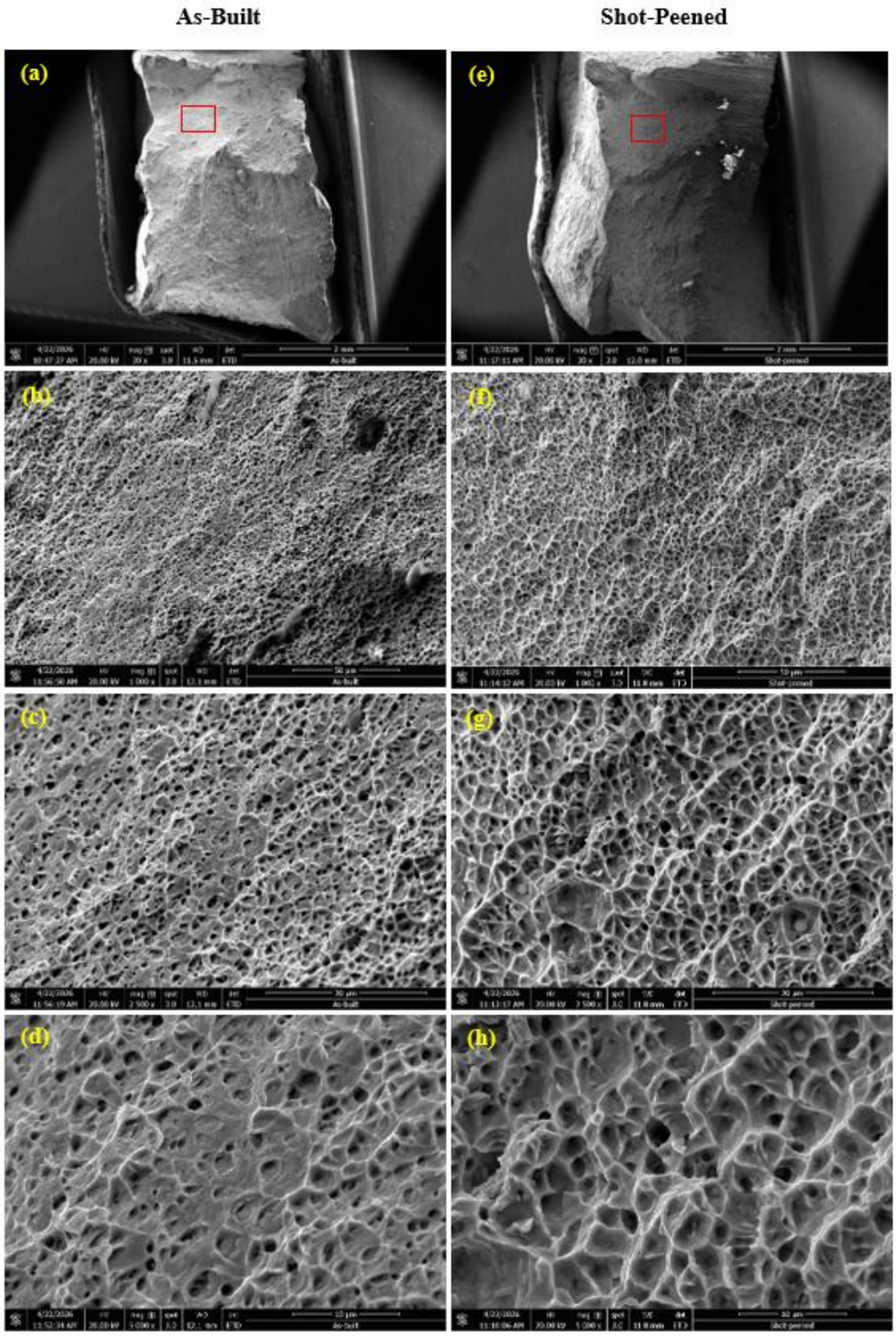


Figure 12. SEM fractography of WAAM 316L SS ; (a) 30x, (b) 1000x, (c) 2500x, and (d) 5000x of as-built specimen; (e) 30x, (f) 1000x, (g) 2500x, and (h) 5000x of shot-peened specimen.

The EDX spectra and elemental maps (Figure 13) that observed in the location as shown in Figure 12(d and h) confirm that both the as-built and shot-peened WAAM-CMT 316L stainless steel specimens are mainly composed of Fe, Cr, Ni, Mo, Mn, and Si, which is consistent with the nominal chemistry of 316L stainless steel. In both conditions, Fe shows the highest peak intensity, while Cr and Ni are the main alloying elements. The presence of Mo is also important because it is one of the key elements responsible for the improved pitting-corrosion resistance of 316L stainless steel. Similar elemental constituents and austenitic stainless-steel chemistry have been reported in WAAM/CMT-WAAM 316L studies, where the deposited material mainly consists of a γ-austenite matrix with residual δ-ferrite formed during solidification**[2, 30]**.

The elemental maps (Figure 13) show that Fe, Cr, Ni, Mo, and Mn are generally distributed throughout the examined regions, indicating that the WAAM-CMT process produced a chemically continuous deposit without obvious elemental discontinuity at the analyzed scale. However, some local variation in contrast can be observed, which may be attributed to mild microsegregation during solidification. In WAAM 316L stainless steel, repeated thermal cycling and relatively slow cooling can promote cellular/dendritic solidification, where Cr and Mo tend to partition toward δ-ferrite or interdendritic regions, while Ni is generally associated with the austenitic matrix. This behavior agrees with previous WAAM 316L studies reporting γ-austenite with residual δ-ferrite and local elemental partitioning caused by the solidification path and reheating during layer-by-layer deposition**[31, 32]**.

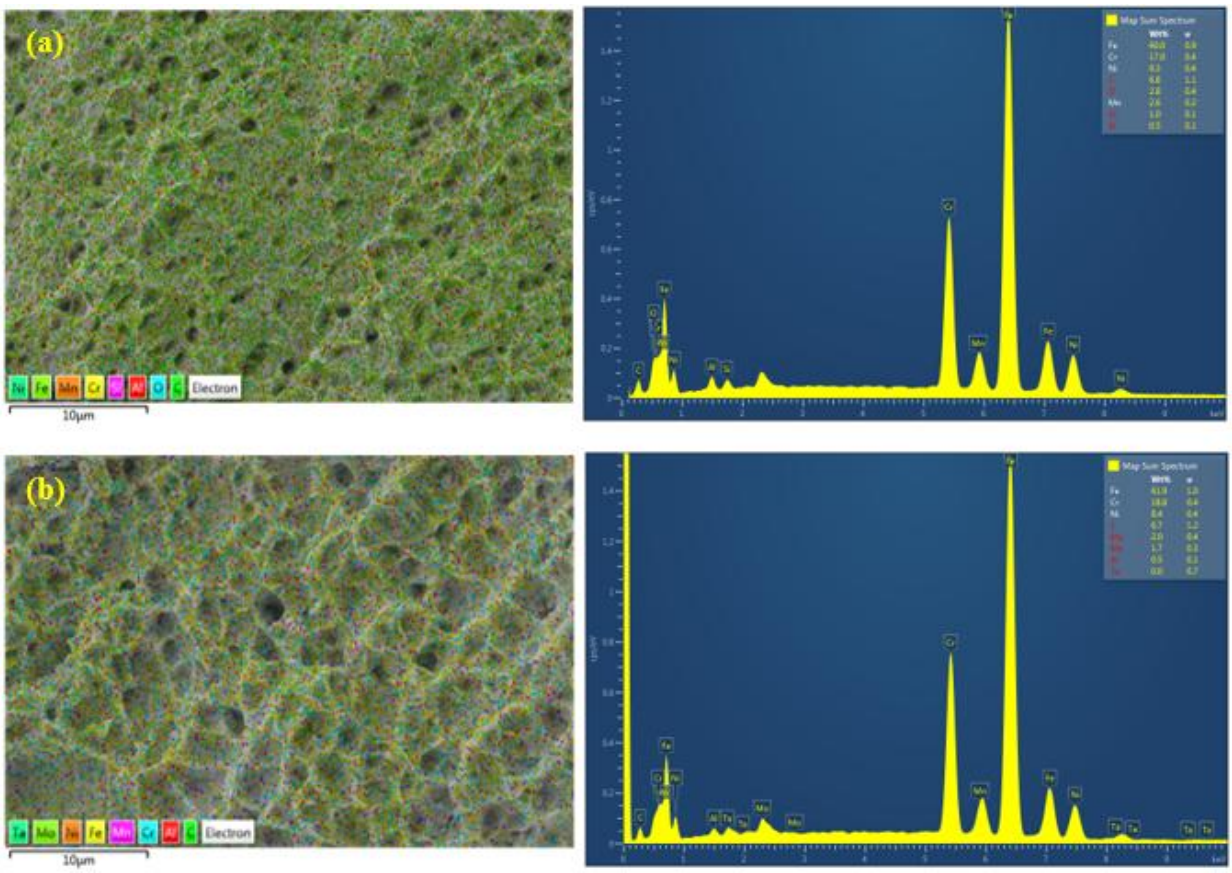


Figure 13. EDX spectra and elemental maps of WAAM-CMT 316L stainless steel ; (a) as-built and (b) shot-peened condition.

Comparison between the as-built and shot-peened specimens shows that shot peening does not significantly change the overall chemical composition as detected by EDX. The main peaks remain Fe, Cr, Ni, and Mo in both spectra, and no new dominant element or contamination peak is observed after treatment. This is expected because shot peening is a mechanical surface-treatment process; it modifies the near-surface condition through plastic deformation, work hardening, and compressive residual stress, rather than changing the alloy chemistry.

A small oxygen signal is visible in the spectra, which may be associated with surface oxidation after WAAM deposition or after sample preparation/shot peening. This is reasonable for stainless steels because Cr-rich passive films can naturally form on the surface. However, the oxygen level appears minor compared with the metallic elements, suggesting that no severe oxidation or thick oxide scale dominates the analyzed surface. The absence of strong foreign-element peaks also indicates that the shot-peening treatment did not cause major surface contamination under the present conditions.

Overall, the EDX analysis confirms that both as-built and shot-peened WAAM-CMT 316L stainless steel retain the expected 316L alloy chemistry. The slight local elemental variation is more likely related to WAAM solidification and thermal-cycle-induced microsegregation than to the shot-peening treatment. Thus, the EDX results support the microstructural and mechanical observations: the WAAM process controls the bulk chemical and microstructural features, while shot peening mainly improves the near-surface mechanical condition without altering the base alloy composition.

4. Conclusions

In this work, the mechanical properties and microstructure of SS316L parts fabricated by CMT-WAAM (Cold Metal Transfer Wire Arc Additive Manufacturing) were analyzed and discussed in detail in the as-built condition and after mechanical surface treatment by shot peening. The main conclusions can be summarized as follows:

- For as-built WAAM-CMT 316L (horizontal), strength is highest at the bottom (~480 MPa UTS) and decreases toward the top, while ductility rises from ~32% to ~40%. Shot peening slightly increases UTS (470–511 MPa) but reduces ductility to ~25–27%, with the largest drop (~45%) in the middle and top regions.
- For shot peened WAAM-CMT 316L (vertical), tensile strength increased but ductility reduced. In V1, UTS rose from 468.08 MPa to 514.26 MPa, with elongation dropping from 32.12% to 26.55%. In V2, UTS increased from 358.59 MPa to 467.91 MPa, while elongation fell from 31.16% to 22.07%.
- The sample from the center of the wall (V1) showed better mechanical performance than the side sample (V2), indicating that part geometry and property gradients affect tensile test results.
- Shot peening of WAAM-CMT 316L induces surface work hardening and compressive stresses, slightly increasing UTS and YS while reducing ductility due to limited plastic deformation and earlier crack initiation.
- In the bottom zone, the as-built microstructure consists of fine, elongated columnar grains with cellular or dendritic substructures from rapid solidification in the WAAM-CMT process. After shot peening, impact-induced plastic deformation refines the near-surface region, producing finer, more equiaxed grains.
- In the middle zone, the as-built microstructure features homogeneous elongated columnar grains with cellular or dendritic substructures, including some coarse grains spanning multiple layers. After shot peening, the near-surface region exhibits pronounced grain refinement compared to the as-built state.
- In the top zone, the as-built microstructure consists of coarse columnar grains aligned with the build direction, larger than in lower zones due to slower cooling. After shot peening,

the near-surface region exhibits refined, more equiaxed grains and a reduced columnar morphology, resulting in a more homogeneous microstructure.

- Microhardness is highest in the bottom section due to fine grains, thermal cycling, and shot-peening stresses; intermediate in the middle section; and lowest in the top section, though all zones show a noticeable microhardness increase after shot peening.
- SEM fractography revealed that both as-built and shot-peened specimens failed mainly through ductile micro-void nucleation, growth, and coalescence.
- EDX analysis confirmed that both as-built and shot-peened specimens retained the expected 316L stainless-steel chemistry, mainly consisting of Fe, Cr, Ni, Mo, Mn, and Si. The shot-peening treatment did not introduce significant compositional changes or contamination.

Author contribution Dr. S Adjel conducted the experimental work, including characterization and testing. Dr. M Boukraa, A Permana, S H Iftikhar conceptualized and guided the thematic framework. Dr. N Merah, F Al-Badour, T Chekifi, A Chibani were involved in the overall paper writing and reviewing the final draft.

Funding No external funding was received. This work was supported by the author's own resources.

Data availability All relevant data are contained within the article and are accessible to the public without restriction.

Declarations

Competing interests The authors declare that they have no known competing fnancial interests or personal relationships that could have appeared to infuence the work reported in this paper

References

[1] G. Kishor, K. K. Mugada, R. P. Mahto, and V. Badheka, “Effect of process conditions on mechanical and metallurgical properties of wire arc additively manufactured 316L stainless steel,” *Journal of Materials Engineering and Performance,* vol. 34, no. 10, pp. 8431-8451, 2025.

[2] S. Kumar Jain, Q. Murtaza, and P. Singh, “CMT AssisTed Wire ArC AddiTive MAnufACTuring of ss 316L: fAbriCATion, ChArACTerizATion, And frACTograPhy,” *Archives of Metallurgy and Materials*, pp. 147-153-147-153, 2025.

[3] S. K. Jain, Q. Murtaza, and P. Singh, “Investigations and multi-response optimization of process parameters for SS316L cold metal transfer-wire arc additive manufactured samples,” *Journal of Materials Engineering and Performance,* vol. 34, no. 10, pp. 8462-8472, 2025.

[4] X. Du, Y. Shen, W. Zhao, J. Chen, R. Liu, and Y. Wei, “Wire arc additive manufacturing from the perspective of remanufacturing: A review of data processing,” *Journal of Manufacturing Processes,* vol. 107, pp. 385-410, 2023.

[5] S. W. Williams, F. Martina, A. C. Addison, J. Ding, G. Pardal, and P. Colegrove, “Wire+ arc additive manufacturing,” *Materials science and technology,* vol. 32, no. 7, pp. 641-647, 2016.

[6] G. Gabriel, F. Al-Badour, N. Merah, R. K. Suleiman, M. Boukraa, and A. Samir, “Friction stir processing of additively manufactured stainless steels: a comprehensive review,” *Progress in Additive Manufacturing*, pp. 1-30, 2026.

[7] S. Li, J. Li, Z. Jiang, Y. Cheng, Y. Li, S. Tang, J. Leng, H. Chen, Y. Zou, and Y. Zhao, “Controlling the columnar-to-equiaxed transition during Directed Energy Deposition of Inconel 625,” *Additive Manufacturing,* vol. 57, pp. 102958, 2022.

[8] A. Hamrani, A. Agarwal, A. Allouhi, and D. McDaniel, “Applying machine learning to wire arc additive manufacturing: a systematic data-driven literature review,” *Journal of Intelligent Manufacturing,* vol. 35, no. 6, pp. 2407-2439, 2024.

[9] R. Li, G. Wang, X. Zhao, F. Dai, C. Huang, M. Zhang, X. Chen, H. Song, and H. Zhang, “Effect of path strategy on residual stress and distortion in laser and cold metal transfer hybrid additive manufacturing,” *Additive Manufacturing,* vol. 46, pp. 102203, 2021.

[10] U. Gürol, E. Kocaman, S. Dilibal, and M. Koçak, “A comparative study on the microstructure, mechanical properties, wear and corrosion behaviors of SS 316 austenitic stainless steels manufactured by casting and WAAM technologies,” *CIRP Journal of Manufacturing Science and Technology,* vol. 47, pp. 215-227, 2023.

[11] U. Gürol, S. Dilibal, B. Turgut, H. Baykal, H. Kümek, and M. Koçak, “Manufacturing and characterizaton of waam-based bimetallic cutting tool,” *International Journal of 3D Printing Technologies and Digital Industry,* vol. 6, no. 3, pp. 548-555, 2022.

[12] D. Ding, Z. Pan, S. Van Duin, H. Li, and C. Shen, “Fabricating superior NiAl bronze components through wire arc additive manufacturing,” *Materials,* vol. 9, no. 8, pp. 652, 2016.

[13] V. Rajkumar, N. S. Shanmugam, N. P. Kumar, K. K. Kumar, and A. R. Kannan, “Microstructure, mechanical properties, and corrosion behaviour of wire arc additive manufactured martensitic stainless steel 410 for pressure vessel applications,” *International Journal of Pressure Vessels and Piping,* vol. 209, pp. 105171, 2024.

[14] S. F. Lone, D. W. Rathod, and S. N. Ahmad, “Exploring the feasibility of SS316L fabrication via CMT-based WAAM: A Comprehensive study on microstructural, mechanical and tribological properties,” *Mechanical Engineering for Society and Industry,* vol. 4, no. 2, pp. 237-251, 2024.

[15] S. KumarJain, Q. Murtaza, and P. Singh, “Microstructural and Mechanical characterization of Wire arc additive Manufactured stainless steel 316l,” *Archives of Metallurgy and Materials*, pp. 119-126-119-126, 2025.

[16] Q. Wang, S. Chen, and L. Rong, “δ-ferrite formation and its effect on the mechanical properties of heavy-section AISI 316 stainless steel casting,” *Metallurgical and Materials Transactions A,* vol. 51, no. 6, pp. 2998-3008, 2020.

[17] S. K. Jain, Q. Murtaza, and P. Singh, “Microstructural and mechanical properties analysis of SS 316L structure fabricated using CMT-wire arc additive manufacturing,” *Journal of Adhesion Science and Technology,* vol. 39, no. 1, pp. 133-153, 2025.

[18] M. R. Zahidin, F. Yusof, S. H. A. Rashid, S. Mansor, S. Raja, M. F. Jamaludin, Y. H. Manurung, M. S. Adenan, and N. I. S. Hussein, “Research challenges, quality control and monitoring strategy for Wire Arc Additive Manufacturing,” *Journal of Materials Research and Technology,* vol. 24, pp. 2769-2794, 2023.

[19] C. Xia, Z. Pan, J. Polden, H. Li, Y. Xu, S. Chen, and Y. Zhang, "A review on wire arc additive manufacturing: Monitoring, control and a framework of automated system," *Journal of manufacturing systems,* vol. 57, pp. 31-45, 2020.

[20] B. Wu, Z. Pan, D. Ding, D. Cuiuri, H. Li, J. Xu, and J. Norrish, "A review of the wire arc additive manufacturing of metals: properties, defects and quality improvement," *Journal of manufacturing processes,* vol. 35, pp. 127-139, 2018.

[21] C.-j. Wang, T. Liu, P. Zhu, Y. Lu, and T. Shoji, "Study on microstructure and tensile properties of 316L stainless steel fabricated by CMT wire and arc additive manufacturing," *Materials Science and Engineering: A,* vol. 796, pp. 140006, 2020.

[22] H. Xu, T. Tian, B. Hua, W. Zhan, L. Niu, B. Han, and Q. Zhang, "Effect of in-situ rolling and heat treatment on microstructure, mechanical and corrosion properties of wire-arc additively manufactured 316L stainless steel," *Journal of Materials Research and Technology,* vol. 27, pp. 3349-3361, 2023.

[23] T. A. Rodrigues, J. Escobar, J. Shen, V. R. Duarte, G. Ribamar, J. A. Avila, E. Maawad, N. Schell, T. G. Santos, and J. Oliveira, "Effect of heat treatments on 316 stainless steel parts fabricated by wire and arc additive manufacturing: Microstructure and synchrotron X-ray diffraction analysis," *Additive Manufacturing,* vol. 48, pp. 102428, 2021.

[24] J. Vora, H. Parmar, R. Chaudhari, S. Khanna, M. Doshi, and V. Patel, "Experimental investigations on mechanical properties of multi-layered structure fabricated by GMAW-based WAAM of SS316L," *Journal of materials research and technology,* vol. 20, pp. 2748-2757, 2022.

[25] G. Thangamani, S. Kumar Tamang, M. S. Patel, J. Arackal Narayanan, M. Thangaraj, J. Zhang, P. Kumar Gianchandani, and P. Iyamperumal Anand, "Studies on the effect of laser shock peening intensity on the mechanical properties of wire arc additive manufactured SS316L," *Journal of Manufacturing and Materials Processing,* vol. 9, no. 1, pp. 8, 2024.

[26] R. Haribaskar, and T. Sampath Kumar, "Surface integrity of consecutive shot-peened additively manufactured 316L stainless steel," *Materials and Manufacturing Processes,* vol. 39, no. 13, pp. 1817-1829, 2024.

[27] T. Rautio, M. Jaskari, T. Gundgire, T. Iso-Junno, M. Vippola, and A. Järvenpää, "The effect of severe shot peening on fatigue life of laser powder bed fusion manufactured 316L stainless steel," *Materials,* vol. 15, no. 10, pp. 3517, 2022.

[28] M. Hietala, T. Rautio, M. Keskitalo, M. Jaskari, and A. Järvenpää, "Analysing the impact of severe shot peening on the fatigue strength of wire arc additively manufactured carbon steel," *Key Engineering Materials,* vol. 982, pp. 15-20, 2024.

[29] W. Jin, C. Zhang, S. Jin, Y. Tian, D. Wellmann, and W. Liu, "Wire arc additive manufacturing of stainless steels: a review," *Applied sciences,* vol. 10, no. 5, pp. 1563, 2020.

[30] B. Xie, J. Xue, and X. Ren, "Wire arc deposition additive manufacturing and experimental study of 316L stainless steel by CMT+ P process," *Metals,* vol. 10, no. 11, pp. 1419, 2020.

[31] C. Penot, J. Wharton, A. Addison, Y. Wang, and Q. Lu, "Interpass temperature effects on WAAM ER316L stainless steel corrosion using potentiostatic pulse tests," *Npj Materials Degradation,* vol. 7, no. 1, pp. 89, 2023.

[32] S. Christin, S. Hill, H. Taheri, and B. Silwal, "Pulsed robotic wire arc additive manufacturing of 316L stainless steel for forging preforms–processing evaluation," *Progress in Additive Manufacturing*, pp. 1-18, 2026.